UM-P-92/84

Associators in generalized Octonionic maps

C. J. Griffin and G. C. Joshi

Department of Physics, University of Melbourne
Parkville Victoria, Australia 3052

September 10, 1992

Generalising previous work, we show that structural transitions are a general property of a large class of octonionic maps. They can thus be used as an indicator of non-associativity in an octonionic map.

1 Introduction

Previously we investigated large iteration limits of the simplest non–linear octonionic map with associator

$$z \to z^2 + c + c(za) - (cz)a, \quad z = z_\mu \mathbf{e}_\mu \in \mathbb{O} \tag{1}$$

The structural form of attracting basins in the octonion–like region was found to qualitatively resemble that those of the pure complex and quaternionic formulations provided a is small. At a large, such structure is destroyed since the basin of attraction to infinity expands to cover the entire region. Interesting behaviour is seen near the cross-over, typically $a \sim 2$, [1] where the basins undergo structural transitions and new octonion–like finite stable attractors emerge which range in complexity from a simple four sphere to ensembles of intricate six dimensional objects [2].

Studies of complex dynamics is considerably more general than the consideration of a single map, dealing with properties of large classes of maps. For a review, see [3].

A next step in the investigation of the octonions is thus to test the applicability and nature of transitions for other maps, considering the degree to which the transition is influenced by the algebraic structure of the map as opposed to the pure presence of an associator.

In this article we focus on the following generalisation of the quadratic map,

$$M : z \to T(z) + c + c(za) - (cz)a = M_\mu \mathbf{e}_\mu \tag{2}$$

An "effective" three dimensional formulation is used to greatly simplify the analysis. Locating stable fixed points in the octonionic region, allows some striking map independent features to be demonstrated.

2 Generalised maps

2.1 $T(z) = z^p$, $p \in \mathbb{I}$

2.1.1 Reducing the map

Consider the component-wise decomposition of powers of the octonion z,

$$\begin{aligned} z^{p+1} &= f_{p+1}\mathbf{e}_0 + \textstyle\sum_i g_{i,p+1}\mathbf{e}_i \\ &= (z_0\mathbf{e}_0 + \textstyle\sum_j z_j\mathbf{e}_j)(f_p\mathbf{e}_0 + \textstyle\sum_i g_{i,p}\mathbf{e}_i) \\ &= z_0 f_p \mathbf{e}_0 + \textstyle\sum_i (z_0 g_{i,n} + z_i f_p + g_{i,p}\sum_j z_j\mathbf{e}_j)\mathbf{e}_i \end{aligned} \tag{3}$$

Equating coefficients of $\mathbf{e}_\mu$ results in eight simultaneous first order difference equations

$$\begin{aligned} &f_{p+1} = z_0 f_p - \textstyle\sum_i z_i g_{i,p} \\ &g_{i,p+1} = z_0 g_{i,p} + z_i f_p + z_j g_{k,p}\epsilon_{jki} \\ &g_{i,0} = 0, \quad f_0 = 1 \end{aligned} \tag{4}$$

where we have introduced the antisymmetric octonion product $\mathbf{e}_i\mathbf{e}_j = \epsilon_{ijk}\mathbf{e}_k$. The initial conditions suggest the solution $g_{i,p} = z_i g_p$, eliminating the ϵ_{jki} term, and reducing the problem considerably to

$$\begin{aligned} f_{p+1} &= z_0 f_p - s\, g_p \\ g_{p+1} &= z_0 g_p + f_p \end{aligned} \tag{5}$$

with $s = \sum_i z_i^2$. The simplification thus far is equivalent to orienting a single imaginary unit along the direction of the imaginary part of z, treating the problem as a purely complex one, and then explicitly reinstating the S^7 symmetry. This allows a solution to be written immediately

$$\begin{aligned} f_p(z_0, s) &= \frac{1}{2}\left[(z_0 + i\sqrt{s})^p + (z_0 - i\sqrt{s})^p\right] = \mathrm{Re}\, T(z_0 + i\sqrt{s}) \\ g_p(z_0, s) &= \frac{1}{2i\sqrt{s}}\left[(z_0 + i\sqrt{s})^p - (z_0 - i\sqrt{s})^p\right] = \frac{1}{\sqrt{s}}\,\mathrm{Im}\, T(z_0 + i\sqrt{s}) \end{aligned} \tag{6}$$

Adding the associator and aligning the imaginary units $\mathbf{e}_1$,$\mathbf{e}_2$ with c and a respectively leads to a compact description of the map with components

$$\begin{aligned} M_0 &= c_0 + f_p \\ M_1 &= c_1 + g_p z_1 \\ M_{2,3} &= g_p z_{2,3} \\ M_{4,6} &= g_p z_{4,6} - 2a_2\, c_1 z_{7,5} \\ M_{5,7} &= g_p z_{5,7} + 2a_2\, c_1 z_{6,4} \end{aligned} \tag{7}$$

Introducing the spherical co-ordinates $z_{\mathbf{quat}} = z_2^2 + z_3^2$, $z_{\mathbf{oct}} = z_4^2 + z_5^2 + z_6^2 + z_7^2$ reduces the map to a four dimensional equivalent sub-map ($\gamma = a_2^2 c_1^2 > 0$)

$$\begin{aligned} z_0 &\to f_p + c_0 \\ z_1 &\to z_1 g_p + c_1 \\ z_{\mathbf{quat}} &\to g_p^2 z_{\mathbf{quat}} \\ z_{\mathbf{oct}} &\to (g_p^2 + 4\gamma) z_{\mathbf{oct}} \end{aligned} \tag{8}$$

which has the universal property $z_{\mathbf{quat}} \to 0$ in the large iteration limit provided $z_{\mathbf{oct}} \neq 0$ (ie: finite octonion-like limit cycles have no quaternionic component). Since it is these limit cycles which give rise to structural transitions, we set $z_{\mathbf{quat}} = 0$ and consider the octonion-like ($z_{\mathbf{oct}} \neq 0$) fixed points of the resulting three dimensional map.

2.1.2 Fixed points

In the large iteration limit there are two classes of octonion-like fixed points,

$$\begin{aligned} z_1 &= \frac{c_1}{1 \pm \sqrt{1 - 4\gamma}} \\ T(z_0 + i\sqrt{s}) &= (z_0 - c_0) \pm i\sqrt{s\,(1 - 4\gamma)} \end{aligned} \tag{9}$$

These equations permit a solution only while $0 < \gamma < \frac{1}{4}$. Although the structure of the map ultimately determines weather a fixed point exists or not, it is amusing to note that solutions z_1 and g_p are entirely determined by the associator — the fact that at least one of these solutions should have this property is obvious by counting degrees of freedom — there are two map dependent functions in a three dimensional space, in a particular set of co-ordinates, one variable should thus be fixed by the nature of the space itself, and this is strongly influenced by the associator.

Although calculating the stability of fixed points is straight forward for any particular p, to facilitate later generalisations, we retain arbitrary f_p and g_p.

Stability is determined by the eigenvalues of the linearised map near a fixed point, which are solutions of the determinant

$$\begin{vmatrix} \frac{\partial f_p}{\partial z_0} - \lambda & \frac{\partial f_p}{\partial z_1} & \frac{\partial f_p}{\partial z_{\mathrm{oct}}} \\ z_1 \frac{\partial g_p}{\partial z_0} & g_p + z_1 \frac{\partial g_p}{\partial z_1} - \lambda & z_1 \frac{\partial g_p}{\partial z_{\mathrm{oct}}} \\ 2 g_p z_{\mathrm{oct}} \frac{\partial g_p}{\partial z_0} & 2 g_p z_{\mathrm{oct}} \frac{\partial g_p}{\partial z_1} & (g_p^2 + 4\gamma) + 2 z_{\mathrm{oct}} g_p \frac{\partial g_p}{\partial z_{\mathrm{oct}}} - \lambda \end{vmatrix} = 0 \qquad (10)$$

The analytic nature of $T(z)$ allows all partial derivatives to be written in terms of $\frac{\partial f_p}{\partial z_0}$ and $\frac{\partial g_p}{\partial z_0}$. It is also helpful to further remove explicit reference to z_{oct} in favour of $s = z_1^2 + z_{\mathrm{oct}}$. With these simplifications, the eigen-equation becomes

$$\begin{aligned} \lambda^3 &- \left(1 + \left(1 + \frac{C}{s}\right) g_p + (1 + C) \frac{\partial f_p}{\partial z_0}\right) \lambda^2 \\ &+ \left((1 + g_p + B) \frac{\partial f_p}{\partial z_0} + \left(1 + \frac{B}{s}\right) g_p + AC\right) \lambda - AB - g_p \frac{\partial f_p}{\partial z_0} = 0 \end{aligned} \qquad (11)$$

with

$$\begin{aligned} A &= \frac{1}{s} \left(\frac{\partial g_p}{\partial z_0}\right)^2 + \left(\frac{\partial f_p}{\partial z_0}\right)^2 \\ B &= z_1^2 (1 - g_p^2) + g_p^2 s \\ C &= z_1^2 (1 - g_p) + g_p s \end{aligned} \qquad (12)$$

Since γ is bounded and small, expansions about the two extremes $\gamma = \frac{1}{4}$ and $\gamma = 0$, should give some idea about the behaviour over the whole region where associativity can have a non-trivial influence.

- $\gamma \sim \frac{1}{4}$

Consider $\gamma = \frac{1}{4} - \epsilon^2$. Referring to equation 11, the product of all three eigenvalues

$$r = \lambda_0\lambda_+\lambda_- = -AB - g_p\frac{\partial f_p}{\partial z_0} \tag{13}$$

allows $\frac{\partial f_p}{\partial z_0}$ to be computed to $O(\epsilon^0)$

$$\frac{\partial f_p}{\partial z_0} = -\frac{r + AB}{g_p} = \mp\frac{1}{2\epsilon}(Ac_1^2 + r) + O(\epsilon^0) \tag{14}$$

for non-singular behaviour at $\epsilon = 0$, require that $Ac_1^2 + r = \pm x\epsilon + O(\epsilon^2)$. With these simplifications, equation 11 reduces to

$$(\lambda - 1)(\lambda^2 + (2r + 2c_1^2 r + \frac{1}{2}x + \frac{1}{2}c_1^2 x)\lambda - 2r) \pm O(\epsilon) = 0 \tag{15}$$

which has an obvious solution $\lambda_+ \sim 1$. An alternating sign in $O(\epsilon)$ ensures that the corrections to λ_+ will always allow $|\lambda_+| < 1$ for one class of fixed points. The quadratic factor may be solved choosing $r = O(\epsilon)$, which provides a consistent set of solutions

$$\lambda_0 = O(\epsilon) \quad \lambda_+ = 1 - O(\epsilon) \quad \lambda_- = -\frac{1}{2}x(1 + c_1^2) + O(\epsilon) \tag{16}$$

Map dependency is introduced in λ_-, and the fixed point attractivity is determined by the supplementary condition $|x| < \frac{2}{1 + c_1^2} + O(\epsilon)$. Fixed points $z^p \sim z - c - \textit{associator}$ are likely to be small $|z| < 1$, with the sum of c and the associator being almost equal to z (large fixed points are likely to iterate towards infinity and are thus unstable). Thus $x \sim pz^{p-1}$ is also likely to be small, certainly $x < O(\epsilon^0)$ which immediately satisfies the inequality, if c_1 is not too large.

- $\gamma \sim 0$

For $\gamma = \epsilon \sim 0$, one fixed point solution z_1 is large, and thus cannot be a consistent finite solution. We focus on the other root $g_p = \sqrt{1 - 4\gamma}$. Expanding equation 11 in ϵ as before yields

$$(1 - \lambda)(\lambda^2 + (r - 2 + As + rs + As^2)\lambda - r) + O(\epsilon) = 0 \tag{17}$$

with solutions

$$\lambda_+ = 1 + O(\epsilon) \quad \lambda_- = 2 - A(s + s^2) + O(\epsilon) \quad \lambda_0 = O(\epsilon) \tag{18}$$

The condition of stability imposed on the map is $\frac{3}{s + s^2} > A > \frac{1}{s + s^2}$, more restrictive than before since we expect both $s \sim |z|^2$ and $A \sim p^2|z^{2p-2}|$ to be small, ie: $A < \frac{1}{s}$.

These simple calculations demonstrate that if a fixed point solution exists near $\gamma = \{0, \frac{1}{4}\}$ for the class of maps considered, then it is quite possibly stable. Moreover, given no further information about the map, the stable fixed point is more likely to exist near $\gamma = \frac{1}{4}$ than $\gamma = 0$, since $\gamma = 0$ prefer the positive branch fixed point solutions and the inequality is considerably more restrictive, whereas $\gamma = \frac{1}{4}$ is not so sensitive on either count. Subject to existence criterion, a structural transition will then be observed in the octonionic region as γ is increased provided the choice of c does not otherwise obscure the effect.

Obviously this argument could be extended to attracting n–cycles, where similar results would be expected, however, in the light of the approximations made thus far, and the exponentially increasing algebraic complexity, it is not likely that such exploits would indicate structural transitions as transparently as the fixed point case.

2.2 $T(z) = \sum_j k_j z^j,\ k_j \in \mathbb{R}$

Generalisation to arbitrary polynomials with real co–efficients is straight forward. The constructions of the previous section were not dependent on the exact nature of $T(z)$. Indeed is f_p and g_p above are replaced by $\sum_p k_p f_p$ and $\sum_p k_p g_p$, $k_p \in \mathbb{R}$. The analysis proceeds unchanged, and the conclusion is modified only in so far as the definitions of x and A. A fixed point structural transition is permitted, probably near $\gamma = \frac{1}{4}$, for some c with the appropriate simple condition satisfied.

$T(z)$ can also contain terms of arbitrary negative integral powers with real coefficients, since equation 6 also holds in this case — a structural transition is permitted, although the exact location of the transition point is not as cleanly specified as before.

Thus, a general Laurent series with real coefficients is permitted structural transitions on the basis of this simple analysis.

2.3 $T(z) = k_j z^j,\ k_j = k_j^0 + k_j^1 \mathbf{e}_1 \in \mathbb{C}$

Generalising the previous discussion to the simplest complex k_j; with the imaginary unit aligned along $\mathbf{e}_1$ is a little more work, but is similarly not difficult. Defining $F^i = \sum_p k_p^i f_p$, $F = F^0 + iF^1$ and similarly for G the four dimensional submap generalises to

$$\begin{aligned} z_0 &\to F^0 - G^1 z_1 \\ z_1 &\to G^0 z_1 + F^1 \\ z_{\text{quat}} &\to (G^{1\,2} + G^{0\,2}) z_{\text{quat}} \\ z_{oct} &\to (G^{1\,2} + G^{0\,2} + 4\gamma) z_{oct} \end{aligned} \tag{19}$$

where c has been absorbed into the definition of $T(z)$. As before, $z_{\text{quat}} \to 0$ for finite octonionic limit cycles after a large number of iterations. The fixed point equations can be

simply stated

$$\begin{aligned} &F(z_0 + i\sqrt{s}) + iz_1 G(z_0 + i\sqrt{s}) = z_0 + iz_1 \\ &|G(z_0 + i\sqrt{s})| = \sqrt{1 - 4\gamma} \end{aligned} \tag{20}$$

In what follows, we assume that such a solution exists.

The role of Non-associativity is to constrain the magnitude of G, which is much less restrictive than the previous case, because there are now two more unspecified map dependent parameters. The net result is that general properties are not so clearly displayed, as we now demonstrate. Substituting

$$\begin{aligned} z_{\rm oct} &= s - z_1^2 \\ G^0 &= \sqrt{1 - 4\gamma}\sin\phi \\ G^1 &= \sqrt{1 - 4\gamma}\cos\phi \\ \gamma &= \tfrac{1}{4}\sin^2(\phi + \theta) \end{aligned} \tag{21}$$

makes the new phase choice explicit, and allows large an small γ expansions to be considered as angle expansions in ϵ, $(\phi, \theta) = \{(\frac{n\pi}{2} + \epsilon, \frac{m\pi}{2} + \kappa\epsilon), n, m \in \mathbb{I}\}$. The resulting stability determinant is a general cubic

$$-\lambda^3 + A\lambda^2 + B\lambda + C \pm O(\epsilon) = 0 \tag{22}$$

with a choice of sign depending on the exact choice of $\{m, n\}$. $O(\epsilon^0)$ solutions are independent of κ and can be either increased or decreased in magnitude by choosing the appropriate branch, as before. For $n + m$ even ($\gamma \sim 0$), A, B and C also depend on the sign choice in the $O(\epsilon)$ term, which factorises the polynomial in the positive branch

$$(1 - \lambda)Q(\lambda) + O(\epsilon) = 0 \tag{23}$$

The structure of $Q(\lambda)$ is not terribly illuminating; in particular, there is no simplification in terms of the product of eigenvalues which was seen previously, however, it is still at least plausible that a fixed point exists near $\gamma = 0$. For $n + m$ odd ($\gamma \sim \frac{1}{4}$), the equation is still a general cubic, which does not have any simple factors. The best we can do is require $\lambda \sim O(\epsilon)$ is a solution which enforces a condition on the structure of the map

$$z_1^2(A^1 + A^0) + z_1(\frac{1}{s} + z_1^2)\left(\frac{\partial G^0}{\partial z_0}\frac{\partial F^1}{\partial z_0} - \frac{\partial F^0}{\partial z_0}\frac{\partial G^1}{\partial z_0}\right) \leq O(\epsilon) \tag{24}$$

It is clear that these kinds of arguments are not as useful in this case.

A more fruitful way of looking at the complex case is to notice that equation 19 is the same as equation 8 with the following identifications

$$\begin{aligned} c_{1,\mathbb{R}} &= F^1_{\mathbb{C}} \\ c_{0,\mathbb{R}} &= -G^1_{\mathbb{C}} z_1 \\ \gamma_{\mathbb{R}} &= \gamma_{\mathbb{C}} + \tfrac{1}{4}G^{1\ 2}_{\mathbb{C}} \end{aligned} \tag{25}$$

The analysis then follows as before; non-associativity makes severe restrictions on the structure of limit cycles in a map independent manner, allowing structural transitions in a wide range of general octonionic maps with complex co-efficients. One obvious difference worth remembering is that the fixed point upper bound on γ is required to be less than 1/4.

3 Examples

After reviewing numerical calculations performed with the quadratic map, we consider a couple of more general examples and demonstrate that structural transitions can indeed be found with similar behaviour to the quadratic case.

3.1 $M_{I,c} : T(z) = z^2$

Previous numerical studies of the behaviour of the quadratic map have shown that the addition of an associator can be seen as a non-trivial adjustment of c_0, which allows the complex Mandelbrot set to be used as a rough guide to locating transitions. Thus, octonion-like fixed point transitions can be found for c_0 on the positive real side of the main cardioid. Transitions can be clearly seen by considering the divergence of iterates in a particular region of space; typically there is a rapid local decrease in the degree of divergence where the basin of attraction will form. The general nature of transitions is actually much richer than has been this. Careful investigation of the fixed point case shows the typical behaviour; the range $\gamma_{\mathrm{min}} < \gamma < \gamma_{\mathrm{max}}$ over which the new behaviour is observed is in general larger than the range where the fixed point is stable. $\gamma_{\mathrm{min}} < \gamma_f$. Indeed the stable structures outside of the point region consist of kinked or even braided loops which evolve smoothly with γ. In agreement with this analysis, the fixed points exist for $\gamma \lesssim \frac{1}{4}$.

In the two-cycle region, the behaviour is even more elaborate, with regions of smooth evolution interrupted by finite cycle behaviour. It is also possible to have two distinct structural transitions at fixed c, and structural transitions which have stable cycles that never collapse onto fixed N-cycles and extended finite cycles with chaotic structure. Refer to [2] for more details.

3.2 $M_{II,c} : T(z) = z^4 + z^2$

According to Sullivan's classification of Fatou sets [4], the attractors of a complex rational map can be determined by considering the dynamics of the "critical points" which are solutions of $\partial T(z)/\partial z = 0$. This map has three critical points; $z = \pm i$, which have identical dynamics — about these points, the map is locally quartic — and $z = 0$ about which the map is locally quadratic. Figure 1 shows the large iterate dynamics of the critical points in

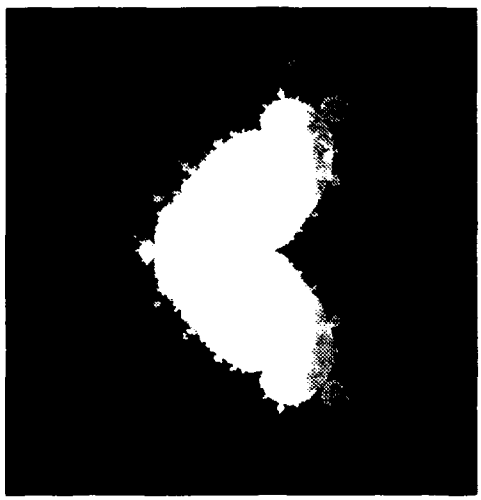

$T(z) = z^4 + z^2$

Figure 1: Large iterate dynamics on the c plane. Colors represent stable regions for different critical points; blue corresponds to the quadratic critical point, and yellow to the quartic critical points, the overlap is rendered white.

the c plane. It is known that the local power law behaviour of a critical point influences the self similar shapes which appear in the c plane [5], which the reason we have explicitly chosen a map with two kinds of critical points. With the aid of figure 1, appropriate choices of c can be made so that structural transitions have a higher probability of being found. We choose $c = -0.54 + 0.066i$, in the one cycle region for both critical points, but near the combined two cycle region, and consider the diversity of attracting basins as γ is evolved. Figure 2 details this progression. For small $\gamma \lesssim 0.012$ a single fixed point basin exists both on the complex plane, and also into the octonionic region. Near $\gamma \sim 0.02$, this basin is destroyed by the associator. Further increasing γ, we see the characteristic swelling which leads to a structural transition at $\gamma \sim 0.027$. The limit cycle has an elaborate structure when it first becomes stable, which then contracts slightly into a kinked ring of similar shape to those seen in quadratic maps in the fixed point region. This is somewhat surprising at first glance, since the fixed point basin has already been destroyed by the associator, and the choice of c is expected to be more amenable to two-cycles. The ring expands and twists as γ is further increased, it's basin of attraction contracting, until the cycle vanishes before $\gamma \sim 0.0305$. There is no associated fixed point for this sequence. Such behaviour is not new, and has actually been seen with the quadratic map, with c chosen from a similar relative position in the Mandelbrot set.

After more swelling, a split two-cycle eventually emerges at $\gamma \sim 0.03975$ which contracts

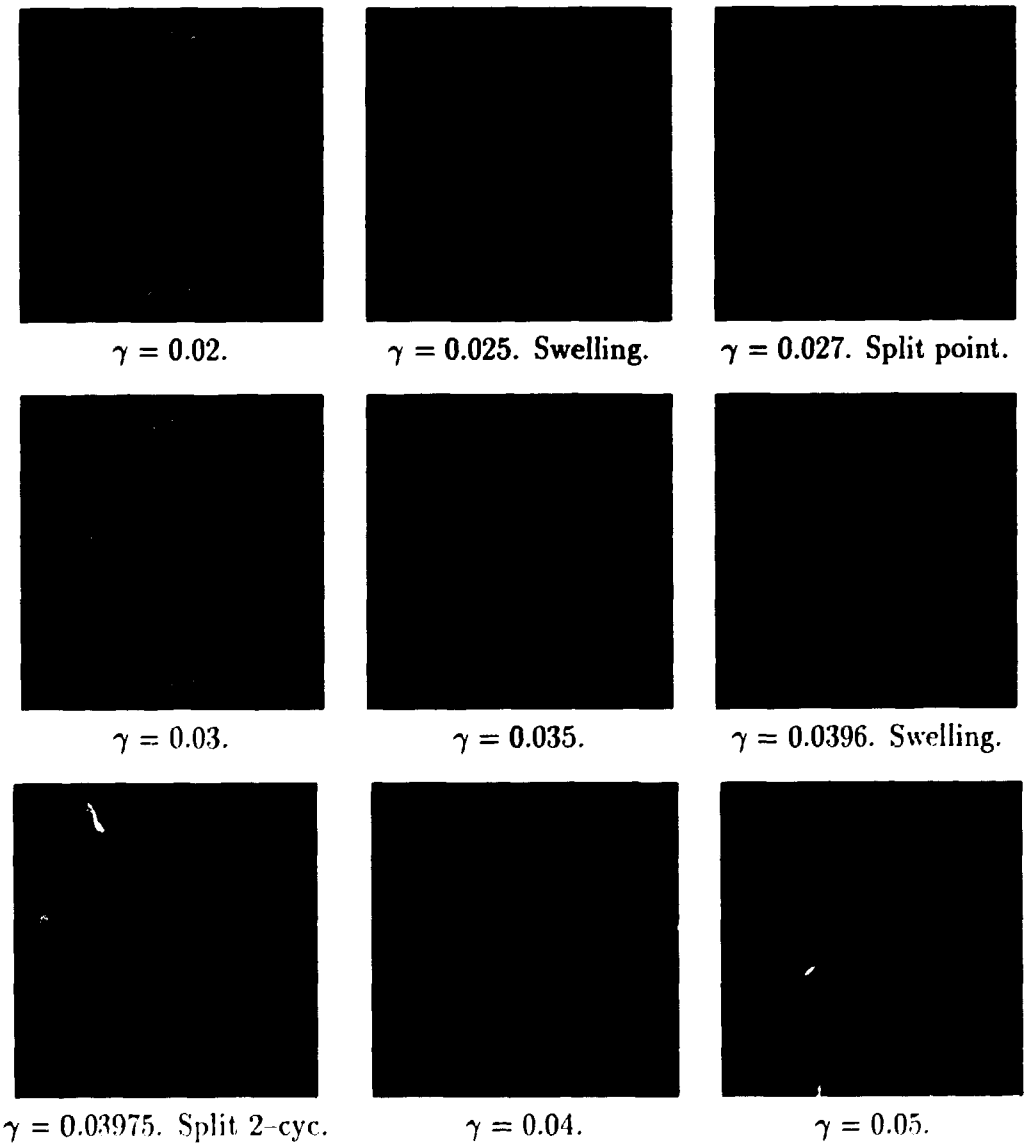

Figure 2: Structural transitions for $T(z) = z^4 + z^2$. (z_0, z_1) plane slice at $z_{\text{oct}} = 0.1$, $c = -0.54 + 0.066i$

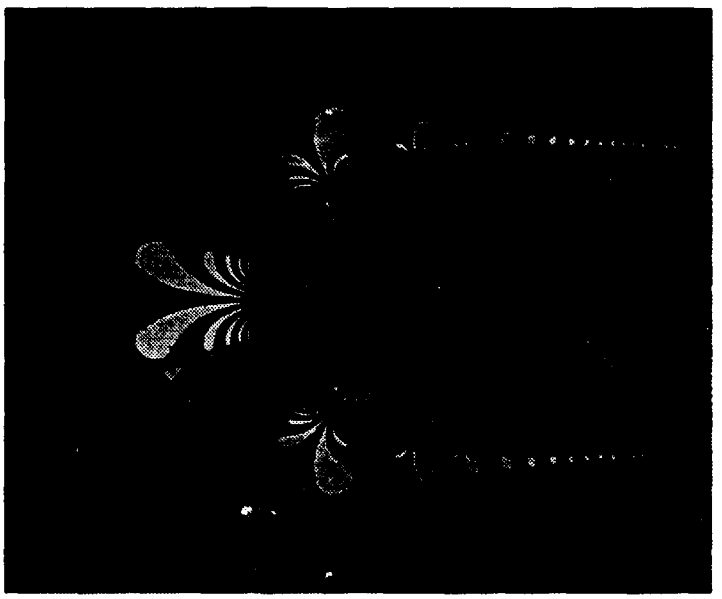

$T(z) = \exp(z)$

Figure 3: Bifurcation set of the complex exponential map. Each color represents a unique periodicity of the limit cycle of $z = 0$

into a regular two-cycle at $\gamma \sim 0.046$, before becoming unstable $\gamma \lesssim 0.05$. Notably, this new limit cycle appears not to have complicated structure. Typically the structure is a pair of loops with a shape that resembles the outline of the two-cycle attractors observed in the pure quadratic map. There observations hints at some sort of universal behaviour for non-associative polynomial maps

3.3 $M_{\mathrm{III},c} : T(z) = \exp(z)$

Exponential maps over the complex field are known to exhibit distinctly different (though similar in some respects) behaviour to rational functions.

For detailed investigation of the dynamics of $x \to \lambda \exp(x)$ for complex x, refer to [6]. There are two classes of Julia sets, $\mathcal{J} = \overline{\mathbb{C}}$, and those which contain Cantour sets of one-dimensional curves.

We make a change of variable $x \to z - c$ with $\exp(c) = \lambda$ which puts the map in the class of polynomials of real coefficients from the point of view of this work. The equivalent of the critical point is $z = 0$. A bifurcation diagram may be constructed in either λ or c space from iterates of this point. A numerical sketch in c space is detailed in figure 3. The change in co-ordinates produces a profile which is only meaningful for c mod $2\pi i$, and is not wrapped around a cardioid as in similar calculations in [6]. The different colored lobes

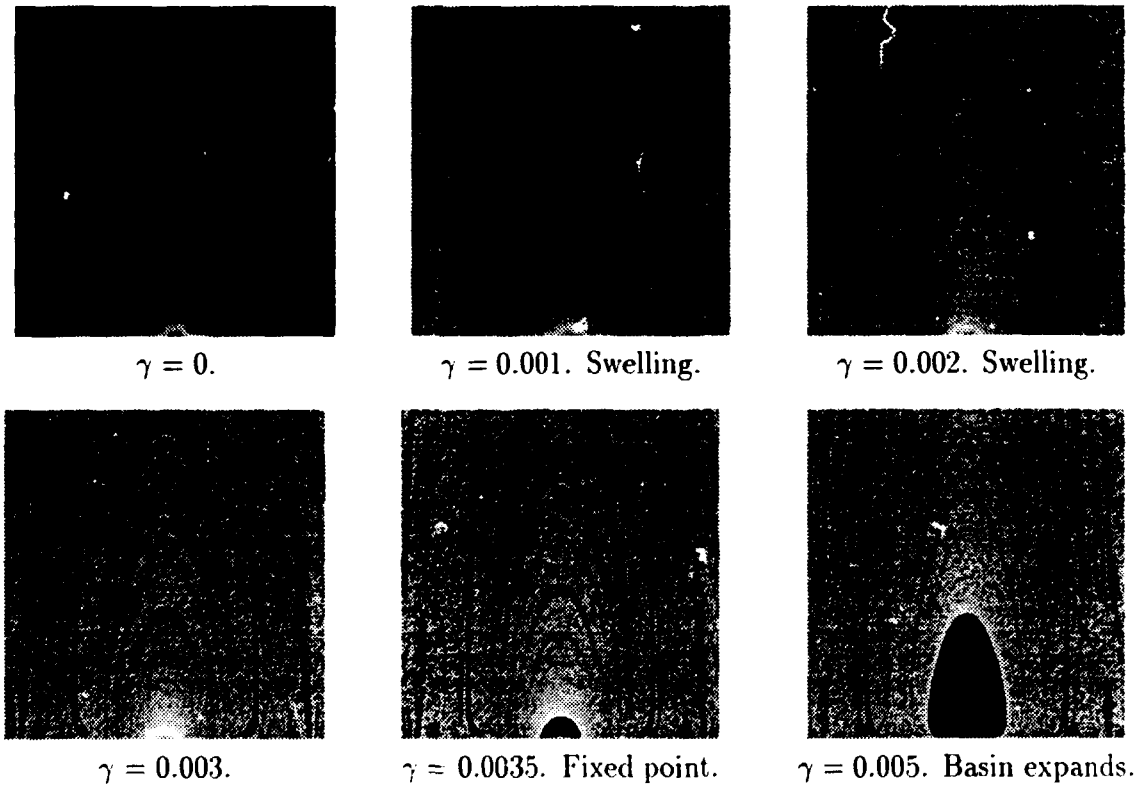

Figure 4: Structural transitions for $T(z) = \exp(z)$. (z_1, z_{oct}) plane slice at $z_0 = 0$, $c = -0.99$

represent different periodicities of finite attractors. Blocks dark regions representing iterates that diverge, are an artifact of machine precision. The regions on which iterates formally diverge are known to be one dimensional "hairs" and are unlikely to be resolved because they are so thin. The simplest hair to locate is the one along the real axis, $z = (-1, \infty)$. As in the rational case, there is a correspondence between points on the bifurcation diagram and the structure of Julia sets. Points on a hair correspond to Julia sets which contain all points in $\overline{\mathbb{C}}$

To look for structural transitions in the Octonionic generalisation, we consider iteration behaviour from a point on a hair. For no non-associativity, there is no finite limit set, and the iterates will diverge to machine precision. If a structural transition occurs in the same way we have investigated previously, a finite cycle should appear at some γ, more likely (if a fixed point) near $\gamma = 0.25$, and vanishing again at $\gamma > 0.25$, which should be easily observed, and clearly makes a radical change to the Julia set. The numerical work sets $c = -0.99$, close to the end of the real axis hair. Although $\text{Im}(c) = 0$ is not compatible with $\gamma \neq 0$ for true octonions, we should none the less see typical behaviour. Figure 4 shows the condensing

process in the (z_1, z_{oct}) plane, with the same features identified previously; after swelling, a finite basin emerges at $\gamma_c \lesssim 0.00324$. This is somewhat unusual, since the basins of attraction on the complex plane are typically of infinite extent and the swolen region usually condenses into an attracting basin all at once. Direct solution of the fixed point equations predicts a transition at $\gamma \gtrsim 0.00324 > \gamma_c$, which is indeed where the fixed point becomes attracting, however, as before, some more elaborate behaviour preceeds the fixed point. For example, a 46-cycle is found at $\gamma = 0.00324$, which strangely does not share the same basin as is the case with polynomial maps. The attracting basin quickly expands as γ is increased to fill most of the plane, before being destroyed at $\gamma = 0.25$.

We have not addressed how the change of variable affected non-associativity. The original map definition is ambiguous over higher than complex number fields due to $[z, c] \neq 0$. It would thus be interesting to look in exactly the same region of parameter space at the original formulation $z \rightarrow \lambda \exp(z)$, which we leave to future investigation.

4 Conclusion

Our results indicate that an associator introduces structural transitions universally in a wide range of polynomial maps. Structural transitions also seem to have universal behaviour in that regions of simple attractive cycles are preceded by more complicated behaviour. At the extreme of γ which is universally determined $\gamma \leq 0.25$ (equality for real maps), attractive cycles vanish suddenly, without a reverse swelling process. This kind of generic behaviour may provide some signature of underlying non-associativity even if the specific mechanism is not completely understood. We have further demonstrated qualitatively some differences in the progress of a structural transition between exponential and simple polynomial maps, the polynomial map producing a more sudden transition than the exponential, which condenses at a small seed and then grows rapidly.

CJG would like to acknowledge helpful discussions with LCL Hollenberg and TC Taucher and the partial support of an AO Cappell scholarship.

References

[1] C.J.Griffin, G.C.Joshi, Octonionic Julia Sets, *Chaos, Solitons & Fractals* **2**, *11-24 (1992)*

[2] C.J.Griffin, G.C.Joshi, Transition points in Octonionic Julia Sets, to appear in *Chaos, Solitons & Fractals* **3***(1992)*

[3] P. Blanchard, Complex analytic synamics on the Riemann sphere, *Bull. Am. Math. Soc.* **11**, *85-141 (1984)*

[4] D.Sullivan, Quasiconformal homeomorphisms and dynamics I,II,III IHES preprints (1983)

[5] B.Mandelbrot, The fractal geometry of nature, Freeman, 1982

[6] M.Misiurewicz, On iterates of $\exp(z)$, *Ergod. Th. & Dynam. Sys.* **1**, *103-106 (1981)*; R.L.Devaney, M.Krych, Dynamics of $\exp(z)$, *Ergod. Th. & Dynam. Sys.* **4**, *35-52 (1984)*

[7] R.L.Devaney, Julia sets and bifurcation diagrams for exponential maps, *Bull. Am. Math. Soc.* **11**, *167-171 (1984)*